Supplementary Information

Mathematical model

Stochastic simulations were carried out based on the interactions and biochemical reactions sketched in Figure 2B of the main text using Gillespie's algorithm (Gillespie, 1977) and custom scripts programmed in FORTRAN. The biochemical reactions and parameters for the stochastic model of the *Pr/Pu* system are the following:

1.- xylR-mRNA transcription from different Pr promoter states

$$\varnothing \xrightarrow{\beta_R \cdot f(R)} m_R \qquad (1)$$

$$\varnothing \xrightarrow{\beta_R \cdot f(R_3)} m_R \qquad (2)$$

$$\varnothing \xrightarrow{\beta_R \cdot f(IHF)} m_R \qquad (3)$$

where β_R is the basal transcription rate from the free *Pr* promoter, and $f(R), f(R_3)$ and $f(IHF)$ are Hill functions accounting for the inhibitory action of Ri, Ra and IHF on the *Pr* promoter (Figure 2). Following standard models of transcription regulation (Bintu *et al.*, 2005), we assume the general form:

$$f(x) = \frac{1 + \frac{x}{f_x \cdot \theta_x}}{1 + \frac{x}{\theta_x}}$$

where θ_x is the threshold for the regulatory action of the species *x* and f_x the fold-change in expression of the regulated species. The basal transcription rates were assumed to be between 35-85 nt/s in exponential phase (Vogel and Jensen, 1994). Specifically, β_R was assigned a value of 80 nt/s to match measured XylR levels in exponential phase (Fraile *et al.*, 2001). Transcription rates in stationary phase were assumed ~2-3 times slower than in exponential phase (Proshkin *et al.*, 2010). Fold-change values for negative autoregulation by Ri/Ra (f_R and f_{R_3} respectively), as well as for IHF repression (f_{IHF}) were taken from experimental observations (Fraile *et al.,* 2001; Silva-Rocha and de Lorenzo, 2011), while thresholds θ_x were set to match the desired response taking into account XylR and IHF levels. All parameter values and references are listed in Table 1 of the main text.

2.- *Translational repression of XylR by Crc*

$$Crc + m_R \xrightarrow{\mu} \varnothing \qquad (4)$$

where μ is the association constant for Crc and *xylR*-mRNA.

3.- *XylR activation/inactivation*

$$3R \xrightarrow{K_R^{on}(mxyl)} R_3 \qquad (5)$$

$$R_3 \xrightarrow{K_R^{off}} 3R \qquad (6)$$

where the effective association constant for Ri dimers (K_R^{on}) depends on the presence of the inducer m-xylene. Here we assume the general Michaelis-Menten form

$$K_R^{on}(mxyl) = k_R \frac{1 + \frac{mxyl}{f_m \theta_m}}{1 + \frac{mxyl}{\theta_m}}$$

where the activation constant in the absence of inducer, k_R, should be very small to account for the fact that expression of *Pu* in non-inducing conditions(*m-xyl* = 0) is practically shut off (Silva-Rocha and de Lorenzo, 2012). The induction strength f_m mainly affects the fold-change observed in *Pu* expression after exposure to *m-xyl* and is adjusted to reproduce experimental observations. The ratio $mxyl/\theta_m$ is chosen large, to reflect the fact that cells are exposed to saturating vapors of *m*-xylene in the induced state. The inactivation constant K_R^{off} modulates the presence of transcription bursts in *xylR*-mRNA, and affects the 'leakage' between the low and high expression peaks of *Pu-GFP* in the bimodal distributions.

4.- *Pu activation/inactivation by XylR*

$$P_u^{off} + R_3 \xrightarrow{K_u^{on}(IHF)} P_u^{on} \qquad (7)$$

$$P_u^{on} \xrightarrow{K_u^{off}} P_u^{off} + R_3 \qquad (8)$$

where the activation rate $K_u^{on}(IHF)$ depends on the amount of the regulator IHF available to the *Pu* promoter, as both IHF and Ri are necessary for *Pu* transcription (Silva-Rocha and de Lorenzo, 2011). Again, we consider a phenomenological activation rate as

$$K_u^{on}(IHF) = k_u \frac{1+\frac{IHF}{f_u \theta_u}}{1+\frac{IHF}{\theta_u}}$$

The dissociation constant K_u^{off} is assumed to be independent of IHF for simplicity. Note that all effects due to IHF binding/unbinding can be included in the effective activation rate $K_u^{on}(IHF)$ by appropriately choosing the parameters. The parameters k_u and K_u^{off} control the induction time of the GFP distributions as well as the transcription bursts in *Pu-GFP* mRNA. In our model, f_u is fixed to mimic the experimental fold-change in *Pu* activity (Valls *et al.*, 2002) while k_u and K_u^{off} are adjusted to reproduce the observed behavior in the stochastic distributions in exponential phase.

5.- *Pu-GFP transcription*

$$P_u^{on} \xrightarrow{\beta_u} P_u^{on} + m_u \qquad (9)$$

6.- *XylR and GFP translation*

$$m_R \xrightarrow{\rho_R} m_R + R \qquad (10)$$

$$m_u \xrightarrow{\rho_u} m_u + GFP \qquad (11)$$

Translation rates may also be 2-3 times slower in stationary phase compared to exponential phase (Proshkin *et al.,* 2010). We considered values in the range 5-20 aa/s, and adjusted XylR translation rate (ρ_R) to achieve the experimentally observed levels in exponential and stationary phases (Fraile *et al.,* 2001).

7.- *mRNA and protein degradation*

$$m_R \xrightarrow{\delta_{mR}} \phi \qquad (12)$$

$$m_u \xrightarrow{\delta_{mu}} \phi \qquad (13)$$

$$R \xrightarrow{\delta_R} \phi \qquad (14)$$

$$GFP \xrightarrow{\delta_{GFP}} \phi \qquad (15)$$

Typical mRNA half-lives in bacteria are between 2-10 min (Bernstein *et al.*, 2002; Taniguchi *et al.*, 2010). Ri and GFP proteins are stable and degradations assumed to be dominated by cell growth and

dilution in exponential phase, $\delta_{R,GFP} \sim \ln 2/\tau_d$, where τ_d is the cell division time, which is about 40 mins (Fonseca *et al.*, 2011).

All these reactions were included into Gillespie's algorithm (Gillespie, 1977) to simulate the stochastic time evolution of the different molecular species. Distributions of *Pu-GFP* levels for different parameters and growth state were obtained running ensembles of 20,000 stochastic trajectories and recording the number of GFP molecules at different induction times. To mimic experimental fluorescence background we added a constant production rate of GFP (100 molec./h).

Parameter fitting

All parameters that were not directly taken from previous experimental data were manually adjusted with the following procedure: First, we estimated some parameters values/ranges using deterministic models (see below). For instance, Crc levels were adjusted in exponential phase to give deterministic (average) values of XylR protein in agreement with previous experimental measurements (Fraile *et al.,* 2001), that is, ~15 Ri dimers. Then, for stationary phase we decreased 4-fold Crc levels, as observed experimentally (Ruiz-Manzano *et al.*, 2005; Silva-Rocha and de Lorenzo, 2011) and readjusted basal transcription/translation rates within physiological ranges to achieve the measured levels of XylR in stationary phase, ~60 Ri dimers (Fraile *et al.,* 2001). To estimate activation/inactivation rates of *Pr* and *Pu* promoters, we note that steady state values of the different molecular species depend only on the ratios K_R^{on}/K_R^{off} and K_u^{on}/K_u^{off}, but the induction *dynamics* (response time after induction with *m*-xylene) is sensitive to the individual rates. We used the experimental induction curve in exponential phase to delimit their values (Figure S1), which were further confirmed by simulation of the stochastic GFP distributions (Figure 3, main text). We note that these rates were unchanged in stationary phase conditions but reproduced equally well experimental induction curves and GFP distributions, validating our estimation.

Deterministic equations

To fit some of the model parameters and compare with the stochastic simulations (Figures 3 and 5), we also implemented a deterministic ordinary differential equation model, that was solved using custom

scripts written in MATLAB 2011 (The Mathworks, Inc.). Reactions (1)-(15) , combined with mass action kinetics, give the following set of ordinary differential equations for the time evolution of species concentrations:

$$\frac{d\,m_R}{dt} = \beta_R\left(\frac{1+R/f_R\theta_R}{1+R/\theta_R}+\frac{1+R_3/f_{R3}\theta_{R3}}{1+R_3/\theta_{R3}}+\frac{1+IHF/f_{IHF}\theta_{IHF}}{1+IHF/\theta_{IHF}}\right)-\mu\cdot Crc\cdot m_R-\delta_{mR}m_R$$

$$\frac{d\,R}{dt} = \rho_R m_R + 3K_R^{off}\cdot R_3 - 3K_R^{on}(mxyl)\cdot R^3 - \delta_R R$$

$$\frac{dR_3}{dt} = K_R^{on}(mxyl)\cdot R^3 + K_u^{off}P_u^{on} - K_R^{off}\cdot R_3 - K_u^{on}(IHF)P_u^{off}\cdot R_3$$

$$\frac{dP_u^{off}}{dt} = K_u^{off}P_u^{on} - K_u^{on}(IHF)P_u^{off}$$

$$\frac{dP_u^{on}}{dt} = K_u^{on}(IHF)P_u^{off} - K_u^{off}P_u^{on}$$

$$\frac{dm_u}{dt} = \beta_u P_u^{on} - \delta_{mu}m_u$$

$$\frac{dGFP}{dt} = \rho_u m_u - \delta_{GFP}GFP \qquad (16)$$

The deterministic rate constants are the stochastic rate constants in Table 1 rescaled by cell volume where needed. Since *Pseudomonas putida* has a volume of ~10^{-15} l, we assume that 1 molecule/cell ~ 1nM.

Model for the lacI^q-Ptrc-xylR *construct*

Expression of *xylR mRNA* is increased and controlled by a *lacI-Ptrc* promoter and the addition of the inducer IPTG. The LacI repressor protein binds to the *lacI* promoter at a site overlapping the binding site of the σ^{70} unit of the RNAP, suppressing transcription from this promoter. LacI is deactivated by IPTG: binding of IPTG to LacI induces a conformational change in the LacI structure, such that the complex LacI-IPTG is unable to bind the *lacI* promoter, and transcription takes place. Within our experimental conditions (addition of IPTG to the cells, incubation during 4h to reach mid-exponential phase and then addition of the *m*-xylene inducer), we may assume that the concentration of LacI repressor protein inside cells has reached stationary levels. Therefore, the concentration of LacI repressor as a function of IPTG can be obtained as (Setty *et al.*, 2003; Yagil and Yagil, 1971):

$$\frac{L}{L_T} = \frac{1}{1+\left(\frac{IPTG}{\theta_{IPTG}}\right)^2} \qquad (17)$$

where L is the concentration of free LacI repressor, L_T the total amount of LacI (free plus LacI-IPTG complex), $IPTG$ the concentration of IPTG inducer and θ_{IPTG} the threshold for LacI inactivation. On the other hand, the action of the LacI repressor on *lacI-Ptrc* transcription can be assumed to follow a Michaelis-Menten kinetics (Ozbudak *et al.*, 2004; Setty *et al.*, 2003). Therefore, reactions (1)-(3) for *xylR* transcription are replaced by

$$\varnothing \xrightarrow{\gamma_R \cdot f(L)} m_R \qquad (18)$$

where the regulation function *f(L)* takes the form

$$f(L) = \frac{1 + \frac{L}{f_L \theta_L}}{1 + \frac{L}{\theta_L}} \qquad (19)$$

Using Eq. (17) in (19), we obtain the transcription rate from the *lacI-Ptrc* promoter directly as a function of the IPTG concentration:

$$\varnothing \xrightarrow{\gamma_R \cdot f(IPTG)} m_R \qquad (20),$$

with

$$f(IPTG) = \frac{1 + \frac{a}{f_L} + \left(\frac{IPTG}{\theta_{IPTG}}\right)^2}{1 + a + \left(\frac{IPTG}{\theta_{IPTG}}\right)^2} \qquad (21)$$

and $a \equiv L_T/\theta_L$.

To estimate the parameters in (20)-(21), we note that Eq. (21) can be related to a simpler regulation function

$$\alpha_R\left(1 + \frac{IPTG}{f_{IPTG} K_{IPTG}}\right)/\left(1 + \frac{IPTG}{K_{IPTG}}\right)$$

with a threshold K_{IPTG} and a fold-change parameter f_{IPTG}, that directly represent the effect of IPTG addition on *xylR mRNA*. To mimic the behavior of the experimental distributions as a function of IPTG concentration, we find that proper threshold and fold-change values for IPTG induction are K_{IPTG} = 75

μM and f_{IPTG} = 1/3 respectively. Then, by choosing a sufficiently large value of *a* (LacI levels in the absence of IPTG well above repression threshold), the values of f_L and θ_{IPTG} can be calculated as

$$f_L = \frac{a}{f_{IPTG}(1+a)-1}, \qquad \theta_{IPTG} = \sqrt{\frac{K_{IPTG}^2 \cdot f_L \cdot (1-c)}{c \cdot f_L(1+a)-(a+f_L)}},$$

where $c \equiv (1+f_{IPTG})/2$. The values of *a,* f_L and θ_{IPTG} are given in Table 1. The basal transcription rate γ_R is chosen to reproduce the experimental observation that in the absence of IPTG, the *lacI-Ptrc* promoter produces a leak expression of ~2-fold that of the native *Pr* promoter (de Lorenzo *et al.*, 1993; Silva-Rocha and de Lorenzo, 2011). To summarize, the simulations for the IPTG induced *lacI-Ptrc-Pu* system were carried out with Eqs. (20)-(21) replacing Eqs. (1)-(3) for the stochastic reactions of *xylR-mRNA* transcription. The rest of the reactions and parameters were left unchanged.

REFERENCES

Bernstein JA, Khodursky AB, Lin PH, Lin-Chao S, Cohen SN (2002). Global analysis of mRNA decay and abundance in *Escherichia coli* at single-gene resolution using two-color fluorescent DNA microarrays. *Proc Natl Acad Sci USA* **99:** 9697-9702.

Bintu L, Buchler NE, Garcia HG, Gerland U, Hwa T, Kondev J *et al* (2005). Transcriptional regulation by the numbers: models. *Curr Opin Genet Dev* **15:** 116-124.

de Lorenzo V, Eltis L, Kessler B, Timmis KN (1993). Analysis of *Pseudomonas* gene products using *lacIq/Ptrp-lac* plasmids and transposons that confer conditional phenotypes. *Gene* **123:** 17-24.

Fonseca P, Moreno R, Rojo F (2011). Growth of *Pseudomonas putida* at low temperature: global transcriptomic and proteomic analyses. *Environ Microbiol Rep* **3:** 329-339.

Fraile S, Roncal F, Fernandez LA, de Lorenzo V (2001). Monitoring intracellular levels of XylR in *Pseudomonas putida* with a single-chain antibody specific for aromatic-responsive enhancer-binding proteins. *J Bacteriol* **183:** 5571-5579.

Gillespie DT (1977). Exact stochastic simulation of coupled chemical reactions. *J Phys Chem* **81:** 2340-2361.

Ozbudak EM, Thattai M, Lim HN, Shraiman BI, Van Oudenaarden A (2004). Multistability in the lactose utilization network of *Escherichia coli. Nature* **427:** 737-740.

Proshkin S, Rahmouni AR, Mironov A, Nudler E (2010). Cooperation between translating ribosomes and RNA polymerase in transcription elongation. *Science* **328:** 504-508.

Ruiz-Manzano A, Yuste L, Rojo F (2005). Levels and activity of the *Pseudomonas putida* global regulatory protein Crc vary according to growth conditions. *J Bacteriol* **187:** 3678-3686.

Setty Y, Mayo AE, Surette MG, Alon U (2003). Detailed map of a *cis*-regulatory input function. *Proc Natl Acad Sci USA* **100:** 7702-7707.

Silva-Rocha R, de Lorenzo V (2011). A composite feed-forward loop I4-FFL involving IHF and Crc stabilizes expression of the XylR regulator of *Pseudomonas putida* mt-2 from growth phase perturbations. *Mol BioSyst* **7:** 2982-2990.

Silva-Rocha R, de Lorenzo V (2012). Stochasticity of TOL plasmid catabolic promoters sets a bimodal expression regime in *Pseudomonas putida* mt-2 exposed to *m*-xylene. *Mol Microbiol* **86:** 199-211.

Taniguchi Y, Choi PJ, Li GW, Chen H, Babu M, Hearn J *et al* (2010). Quantifying *E. coli* proteome and transcriptome with single-molecule sensitivity in single cells. *Science* **329:** 533-538.

Valls M, Buckle M, de Lorenzo V (2002). *In vivo* UV laser footprinting of the *Pseudomonas putida* sigma 54Pu promoter reveals that integration host factor couples transcriptional activity to growth phase. *J Biol Chem* **277:** 2169-2175.

Vogel U, Jensen KF (1994). The RNA chain elongation rate in *Escherichia coli* depends on the growth rate. *J Bacteriol* **176:** 2807-2813.

Yagil G, Yagil E (1971). On the relation between effector concentration and the rate of induced enzyme synthesis. *Biophys J* **11:** 11-27.

Supplementary Figure S1. Activation/deactivation rates of XylR and *Pu* promoter (control induction times)

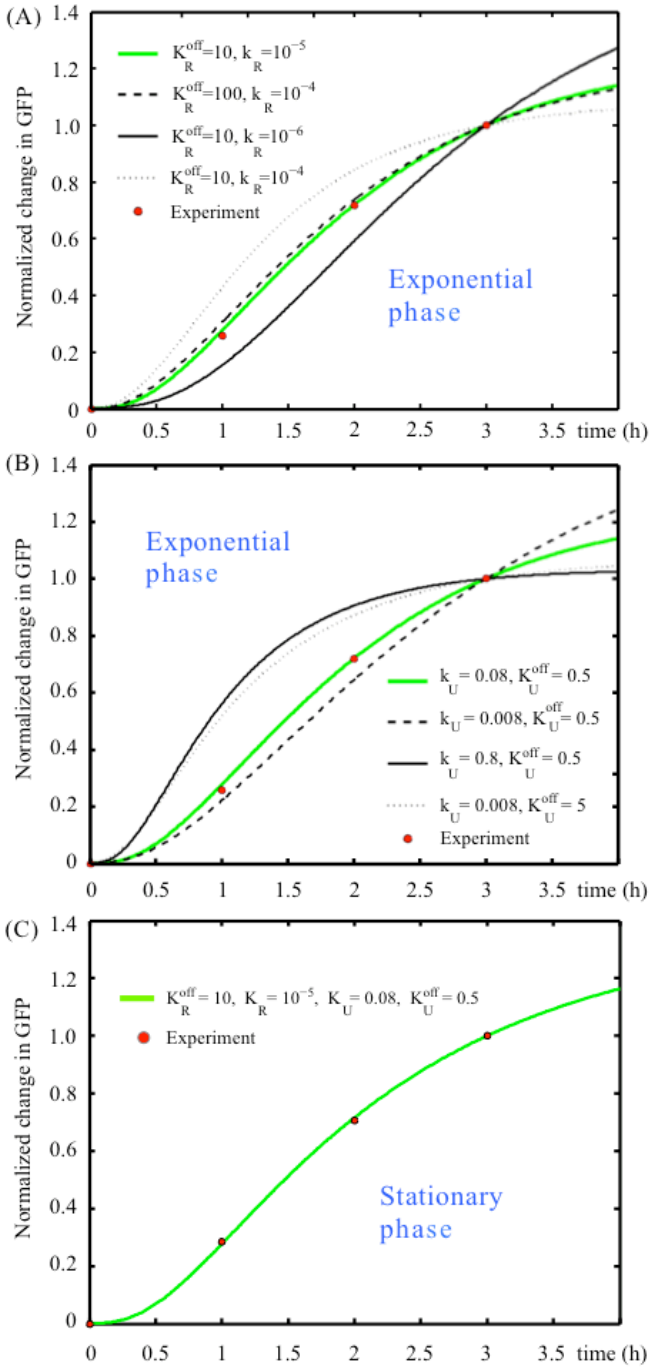

To allow for a comparison between experimental fluorescence intensities and numerical GFP levels, the induction response is obtained as the normalized fold-change in mean GFP level as a function of time. Red dots correspond to the experimental values, while curves are the result of simulations using the deterministic model (Materials and Methods). (A) Effect of activation/deactivation rates for XylR (parameters K_R and K_R^{off} respectively) on the induction response in exponential phase. (B) Effect of activation/deactivation rates of the *Pu* promoter due to Ra (parameters K_U and K_U^{off} respectively) on the induction times in exponential phase. Green lines are obtained with the values used in all stochastic simulations, shown in Table 1. (C) These parameters were adjusted in exponential phase, but reproduced the experimental induction response also in stationary phase

Supplementary Figure S2. Releasing post-transcriptional repression of XylR reduces variability in exponential phase.

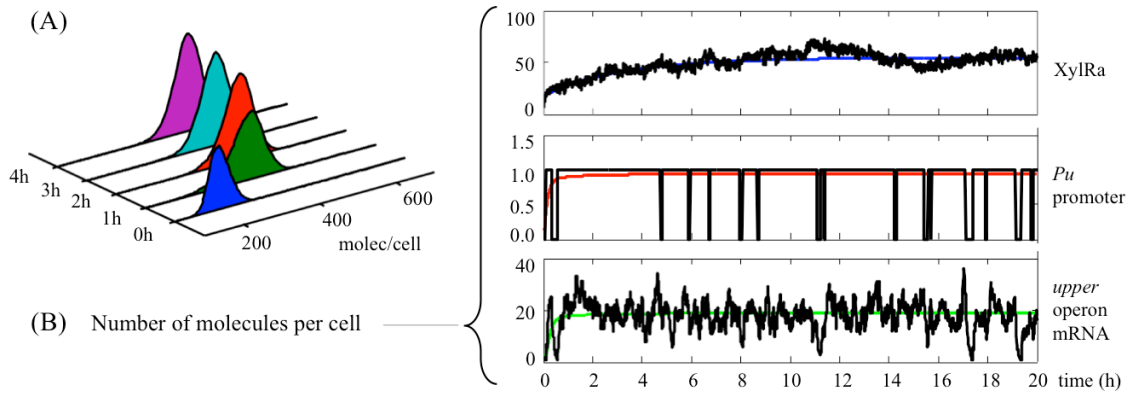

(A) Stochastic distributions of *Pu-GFP* levels in exponential phase conditions, except that Crc abundance is decreased 4-fold (to the levels found in stationary phase). (B) Typical stochastic trajectories showing the increase in active XylR (top panel, blue line is the average value) due to the release of post-transcriptional repression by Crc. The *Pu* promoter undergoes relatively frequent inactivation events but of very short duration (mid panel). This implies that *Pu mRNA* fluctuations are fast and population responses unimodal.